remote sensing

MDPI

Technical Note

A Remote Sensing Perspective on Mass Wasting in Contrasting Planetary Environments: Cases of the Moon and Ceres

Lydia Sam and Anshuman Bhardwaj *

School of Geosciences, University of Aberdeen, Meston Building, King's College, Aberdeen AB24 3UE, UK; lydia.sam@abdn.ac.uk

* Correspondence: anshuman.bhardwaj@abdn.ac.uk

Abstract: Mass wasting, as one of the most significant geomorphological processes, contributes immensely to planetary landscape evolution. The frequency and diversity of mass wasting features on any planetary body also put engineering constraints on its robotic exploration. Mass wasting on other Solar System bodies shares similar, although not identical, morphological characteristics with its terrestrial counterpart, indicating a possible common nature for their formation. Thus, planetary bodies with contrasting environmental conditions might help reveal the effects of the atmosphere, subsurface fluids, mass accumulation/precipitation, and seismicity on mass wasting, and vice versa. Their relative positions within our Solar System and the environmental and geophysical conditions on the Moon and the dwarf planet Ceres are not only extremely different from Earth's but from each other too. Their smaller sizes coupled with the availability of global-scale remote sensing datasets make them ideal candidates to understand mass wasting processes in widely contrasting planetary environments. Through this concept article, we highlight several recent advances in and prospects of using remote sensing datasets to reveal unprecedented details on lunar and Cerean mass wasting processes. We start with briefly discussing several recent studies on mass wasting using Lunar Reconnaissance Orbiter Camera (LROC) data for the Moon and Dawn spacecraft data for Ceres. We further identify the prospects of available remote sensing data in advancing our understanding of mass wasting processes under reduced gravity and in a scant (or absent) atmosphere, and we conclude the article by suggesting future research directions.

Keywords: planetary remote sensing; mass wasting; mass movement; the Moon; Luna; Ceres; landslides; landscape evolution; Lunar Reconnaissance Orbiter Camera (LROC); Dawn spacecraft

Citation: Sam, L.; Bhardwaj, A. A Remote Sensing Perspective on Mass Wasting in Contrasting Planetary Environments: Cases of the Moon and Ceres. *Remote Sens.* **2022**, *14*, 1049. https://doi.org/10.3390/rs14041049

Academic Editors: Jungrack Kim, Sungkoo Bae and Shih-Yuan Lin

Received: 20 January 2022
Accepted: 18 February 2022
Published: 21 February 2022

1. Introduction

Mass wasting or mass movement is bulk downslope movement of rock debris and/or regolith under the influence of gravity [1,2]. Mass wasting contributes immensely to landscape evolution of a planetary body not only through subaerial modifications, but even through subsurface and underwater modulations (e.g., [3–9]). In fact, mass movements are one of the most significant geomorphological processes molding the surface of our planet [10–13]. Interestingly, widely varying mass wasting features have also been identified on other planetary bodies such as the Moon (e.g., [14]), Mercury (e.g., [15]), Venus (e.g., [16]), Mars (e.g., [17–21]), and some outer Solar System satellites (e.g., [22]). Planned instruments to fly to Venus such as the Venus Interferometric Synthetic Aperture Radar (VISAR) onboard VERITAS and the high-resolution imaging capabilities of EnVision are particularly aimed at studying topography and mass movements on Venus [23]. In a terrestrial context, classification schemes for mass wasting usually consider different parameters, such as type of movement (fall, topple, creep, slide, and flow), material involved (rock, regolith, ice, snow, and mixed debris), rate of movement (rapid or slow), and proportion of water, air, rock, and ice in wasted material [24,25]. Thus, mass wasting represents a resultant of all

the interactions among various geomorphological agents and processes, which act with varied intensities on all types of slopes to modify the topography [24,26].

Although gravity is a major requirement for driving mass movement, its isolated effect on the scales and dynamics of mass wasting is hard to investigate by studying terrestrial landslides only, due to the presence of several other ambient factors on Earth, including a dense atmosphere, precipitation, and seismicity. Mass movements on other Solar System bodies share similar, although not identical, morphological characteristics with terrestrial landslides, indicating a possible common nature for their formation. Thus, planetary studies with variable environmental conditions might help reveal the effects of the atmosphere, subsurface fluids, precipitation, and seismicity on mass wasting, and could foster an understanding of triggering and propagation mechanisms. This argument forms the motivation and premise for this concept article. Characterization and comparison of mass wasting features, based on the mass movement type and size, and their global distribution on a planetary body can help us understand the local physical and environmental conditions on surface/subsurface [15]. Figure 1 shows one such example of distribution of several mass wasting features on the Moon.

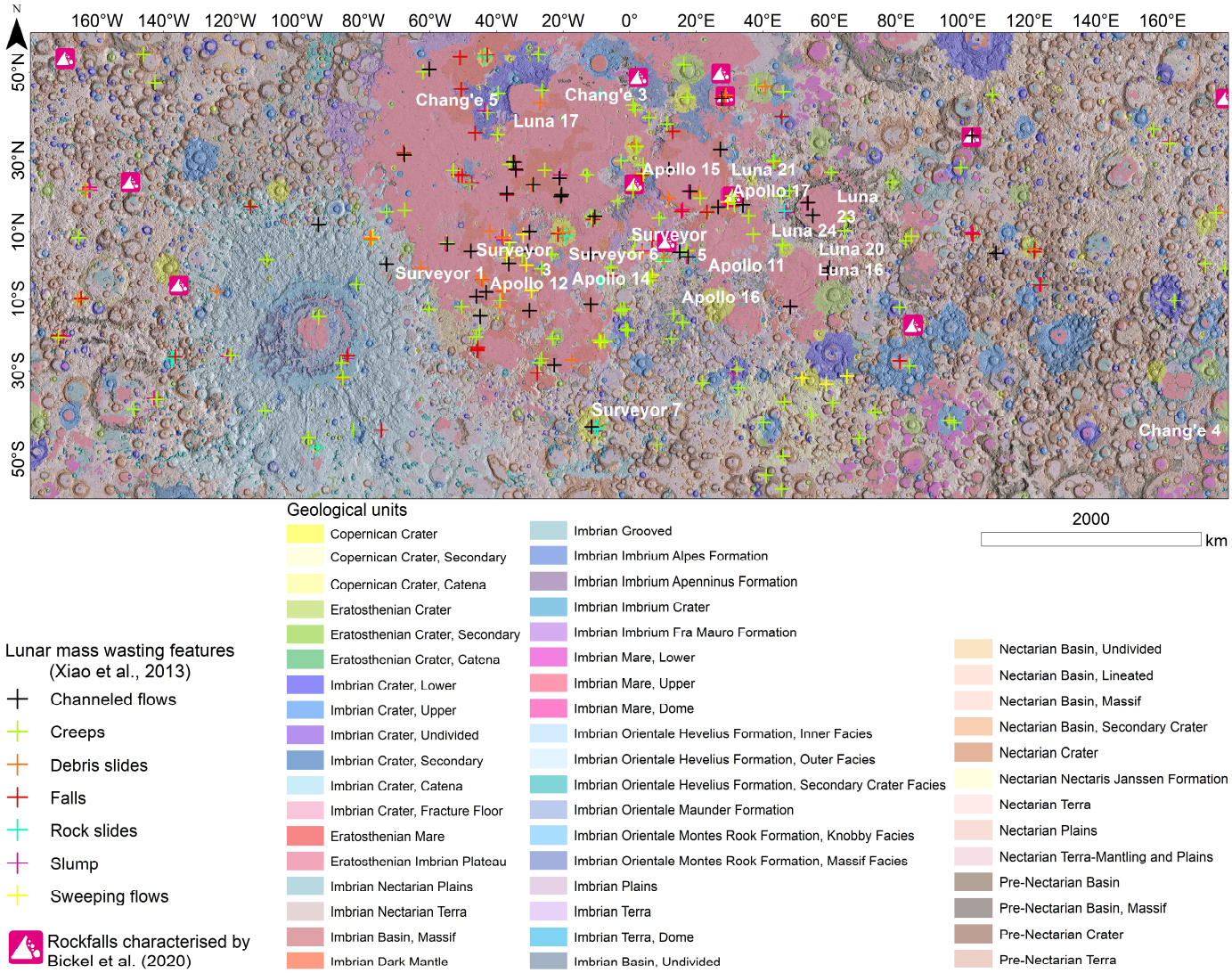

Figure 1. Spatial distribution of lunar mass wasting processes with respect to lunar geology. This map was created using data from various sources. The tabulated data on a variety of lunar mass wasting features from the Supplementary Material of Xiao et al. [2] were plotted in Geographic Information System (GIS). The data on several characterized lunar rockfalls [27] were downloaded from ETH Zurich's Research Coll-

ection [28] and plotted in GIS. The latest data of the Unified Geologic Map of the Moon were obtained from the United States Geological Survey's webpage [29,30]. The landing sites of several lunar missions have been included in the white text to provide the contextual information.

Multiresolution and multisensory remote sensing datasets for planetary bodies are constantly improving our understanding of the Solar System [20]. While terrestrial planets, i.e., Mercury, Venus, Earth, and Mars, have considerable gravity (i.e., ~3.7 m/s^2) to support widespread mass wasting, over the past decade mass wasting features have been observed even in remote sensing images of smaller planetary bodies such as the Moon and Ceres, with considerably lower gravity (i.e., 1.62 m/s^2 for the Moon and 0.27 m/s^2 for Ceres). The Moon is also unique in the Solar System as the only body, other than the Earth, for which we have dated rock samples with an established geological context. Therefore, the landscape evolution through lunar mass wasting can be directly correlated to respective geological ages. The scarce atmosphere and the lesser control of external triggering factors on the Moon and Ceres make them ideal testbeds to study mass wasting under gravity and environmental scenarios that are extremely different from the terrestrial planets. The smaller sizes of both these planetary bodies have also ensured a better availability of repeat medium-to-high resolution remote sensing images [31], allowing us to infer spatiotemporal diversity in mass wasting. However, more importantly, Ceres and the Moon are not only distinct from the terrestrial planets but are also very different from each other in several physical and geological aspects, thus acting as analogues for several other small planetary bodies with contrasting environments. The dwarf planet Ceres is the largest object in the asteroid belt between Mars and Jupiter. It is the only dwarf planet located in the inner solar system, far from not only the Sun but also the Moon. Ceres has a distinct shape of a flattened sphere, and its volume is only ~27% that of the Moon. Ceres rotates fully around its axis every 9 h, compared with the ~27 days taken by the Moon. While in addition to moonquakes, a scant presence of gases surrounding the Moon has been confirmed, there is still no definite evidence of an atmosphere or seismicity on Ceres. In addition to all the aforementioned reasons for considering the Moon and Ceres as ideal cases to understand mass wasting in contrasting planetary environments, a renewed interest in Moon exploration [32] and an interest in considering Ceres as an analogue for icy dwarf planets/asteroids/moons based on several recent findings [33] further warrant understanding their surface processes and landscape evolution.

2. Lunar Mass Wasting Processes: Status and Prospects

Since the era of Apollo missions, mass wasting has been identified as a widespread and predominant geomorphological process on the Moon (e.g., [34,35]). However, the research on this topic was not very holistic in the previous decades owing to the unavailability of high-resolution global-scale remote sensing datasets. This is the reason why, even today, we are uncertain of the relative significance of mass wasting compared with other lunar surface processes, or of their combined effect, on the landscape evolution of the Moon [2]. The focus shifted to exploring the lunar mass wasting processes after the launch of the Lunar Reconnaissance Orbiter Camera (LROC) in 2009. The LROC has two Narrow-Angle Cameras (NACs), designed to provide as high as 0.5 m/pixel panchromatic images over a 5 km swath, and, by now, a major part of the lunar terrain has been imaged by NACs [31]. Free-of-cost and user-friendly planetary data visualisation tools, such as the Java Mission-planning and Analysis for Remote Sensing (JMARS) tool developed by Arizona State University [36], have also been extremely helpful in encouraging quick and efficient geomorphological analyses.

2.1. Status of Our Understanding

Lunar avalanches are believed to involve only dry granular movement, and therefore can reveal the predominant mass wasting processes and flow-deposit morphologies in the absence of liquid and gas [14]. Based on several sample-based studies focusing on selected craters (e.g., [14]) or depending on the availability of high-resolution images

(e.g., [2]), the main types of reported lunar mass movements include debris falls/rockfalls, dense frictional debris flows, slides, slumps, and creep. In the earlier years of lunar exploration, it was believed that mass wasting on the Moon, in the absence of liquid water or atmospheric gas, is predominant on crater slopes and involves some proportion of fine-grained regolith [35,37]. In recent years, several high-resolution remote-sensing-based studies (e.g., [2,14,27]) have confirmed these beliefs and have provided useful insights into the process and distribution of lunar mass wasting. In fact, by sourcing supplementary information from these papers, we have generated a lunar mass wasting distribution map (Figure 1) with various characterized events overlaid on the latest global geology [30]. Moreover, experiments and simulations suggest that dry granular mass wasting is possible even under low lunar gravity (~0.16 g) as the lunar gravity decreases the dynamic angle of repose too [38]. Thus, there is a significant scope in studying a large population of lunar mass movements to better understand the involved processes and landscape evolution under reduced gravity and limited geomorphic agents.

As the first of such global-scale studies within the past decade, Xiao et al. [2] sampled over 300 lunar mass wasting features to study their morphological, evolutionary, formational, distributional, and erosional characteristics. They adopted a comparative planetology approach and interpreted lunar mass wasting in view of its terrestrial or Martian counterparts. A schematic representation of the mass wasting commonly observed on the Moon is given in Figure 2, while Figure 3 shows several examples of the lunar mass wasting in high-resolution LROC-NAC images. Using pre-LROC era geological interpretations by Losiak et al. [39] and Wilhelms et al. [40], Xiao et al. [2] also provided some qualitative inferences on the stratigraphic ages of the host terrains of the mass wasting features. For example, they observed that unlike other mass movements, creeps were present on terrains of all the ages, and more profoundly on older terrains that are covered by relatively thick regolith. Here, we used the latest and highest-resolution global geologic data of the Moon, provided by the United States Geological Survey (USGS) [30], to quantify the prevalence of various mass wasting features [2] in different geologic units (Figure 4). We observed that ~41% of creeping features were observed on Imbrian terrain followed by Eratosthenian (~28%) and Nectarian (~18%). Xiao et al. [2] further reported that they could not observe rockslides, sweeping flows, or channeled flows on terrain older than Eratosthenian. Xiao et al. [2] attributed this observation to the association of slide and flow source material with impact melt, which is less prevalent on terrains older than Eratosthenian. Xiao et al. [2] also asserted that surfaces older than Eratosthenian may no longer have steep enough slopes to form slides and flows due to continuous mass wasting of the older terrain. However, using the updated geologic data [30], we observed that while over ~90% of slides and sweeping flows and ~68% of channeled flows are found on Copernican and Eratosthenian, the remainder of these features are also present on older terrain. For example, ~30% of channeled flows and a majority of the remaining rockslides and sweeping flows can be observed on Imbrian terrain, mostly in the geologic units represented by smooth and fine-textured regolith (e.g., the Upper Mare Unit, the Plains Unit, and the Terra Unit), consistent with the textural property of slides and flows [2]. Similarly, Xiao et al. [2] also mentioned that falls, debris slides, and slumps were prevalent in Copernican and Eratosthenian craters. We quantify that ~70% of falls, ~81% of debris slides, and ~85% of slumps are present in Copernican and Eratosthenian craters. However, we made an interesting observation regarding the geologic units prevalent in mass wasting features. While the steep Copernican Crater Unit and the Eratosthenian Crater Unit had a majority of the mass wasting features, the only other geologic unit showing all types of mass wasting features was the relatively gently sloped Imbrian Upper Mare Unit, probably because this unit is full of numerous small ridges [30], thus showing the control of local topography on lunar mass wasting. This also confirms the notion of Xiao et al. [2] that with the availability of more detailed remote sensing datasets, the known age distribution for lunar mass wasting features might be updated. Xiao et al. [2] further attributed meteor impacts and moonquakes as the reasons behind the formation of the majority of the lunar mass wasting features.

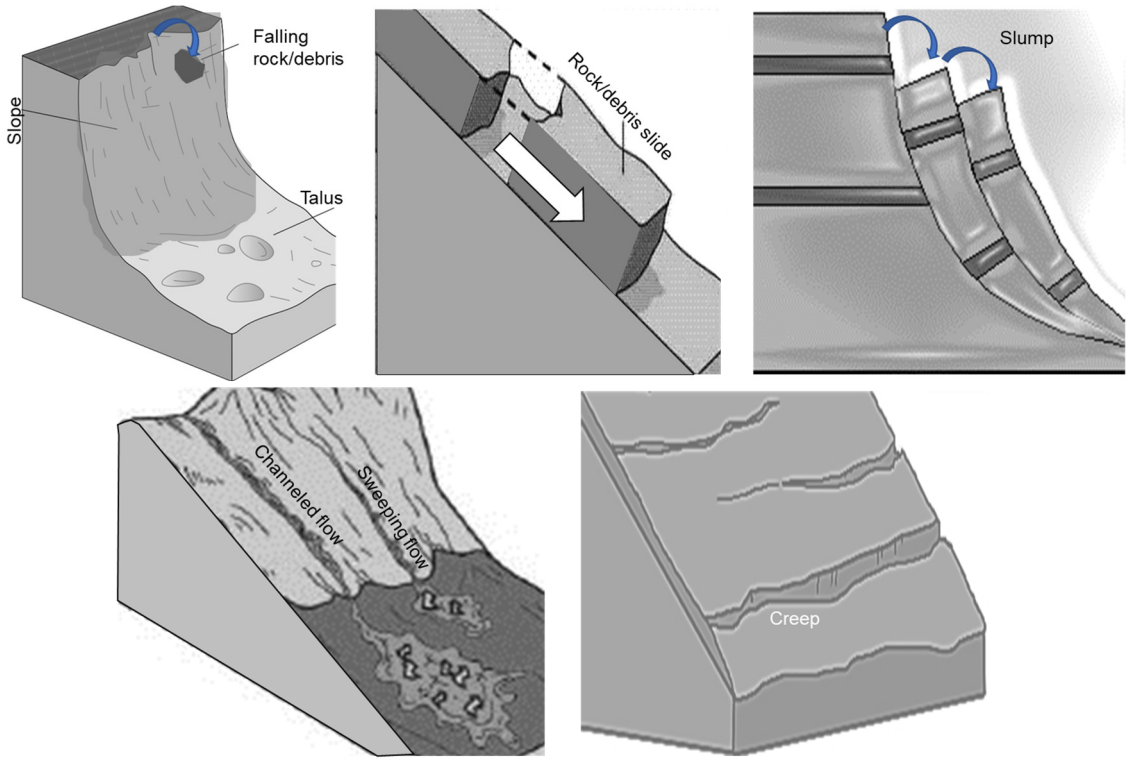

Figure 2. Schematic representation of various mass wasting processes commonly observed on the Moon.

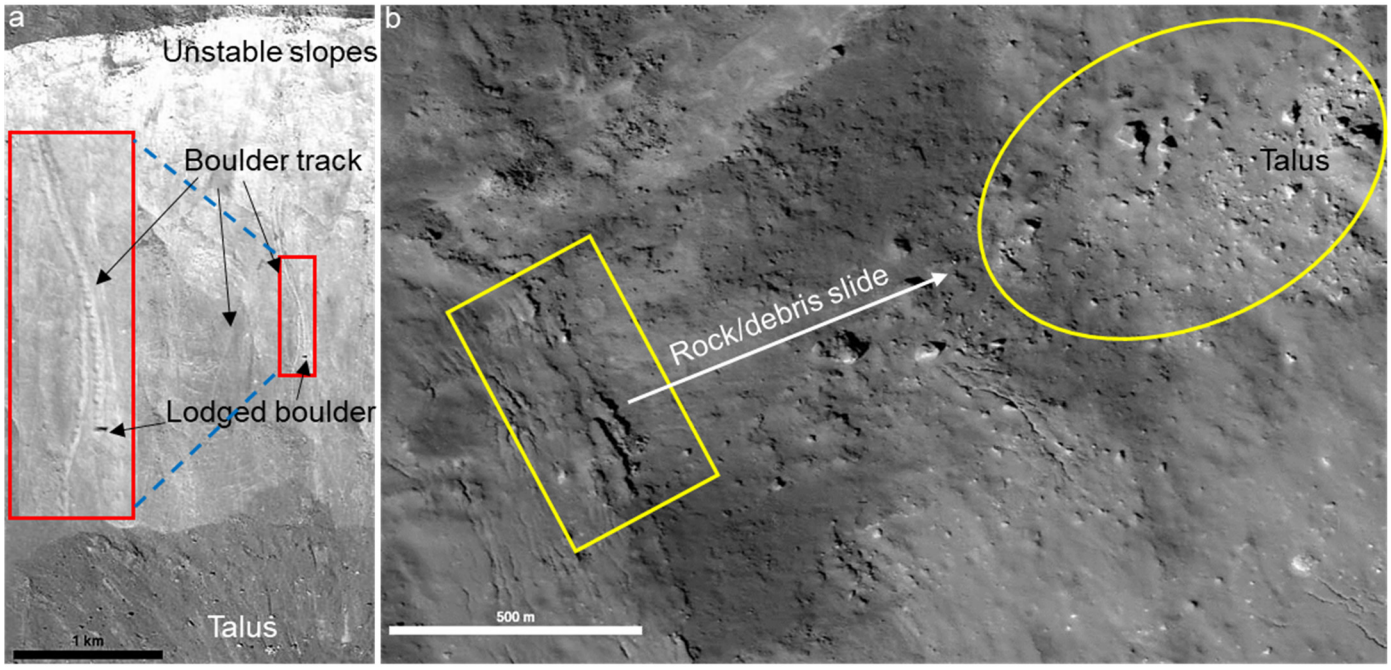

Figure 3. *Cont.*

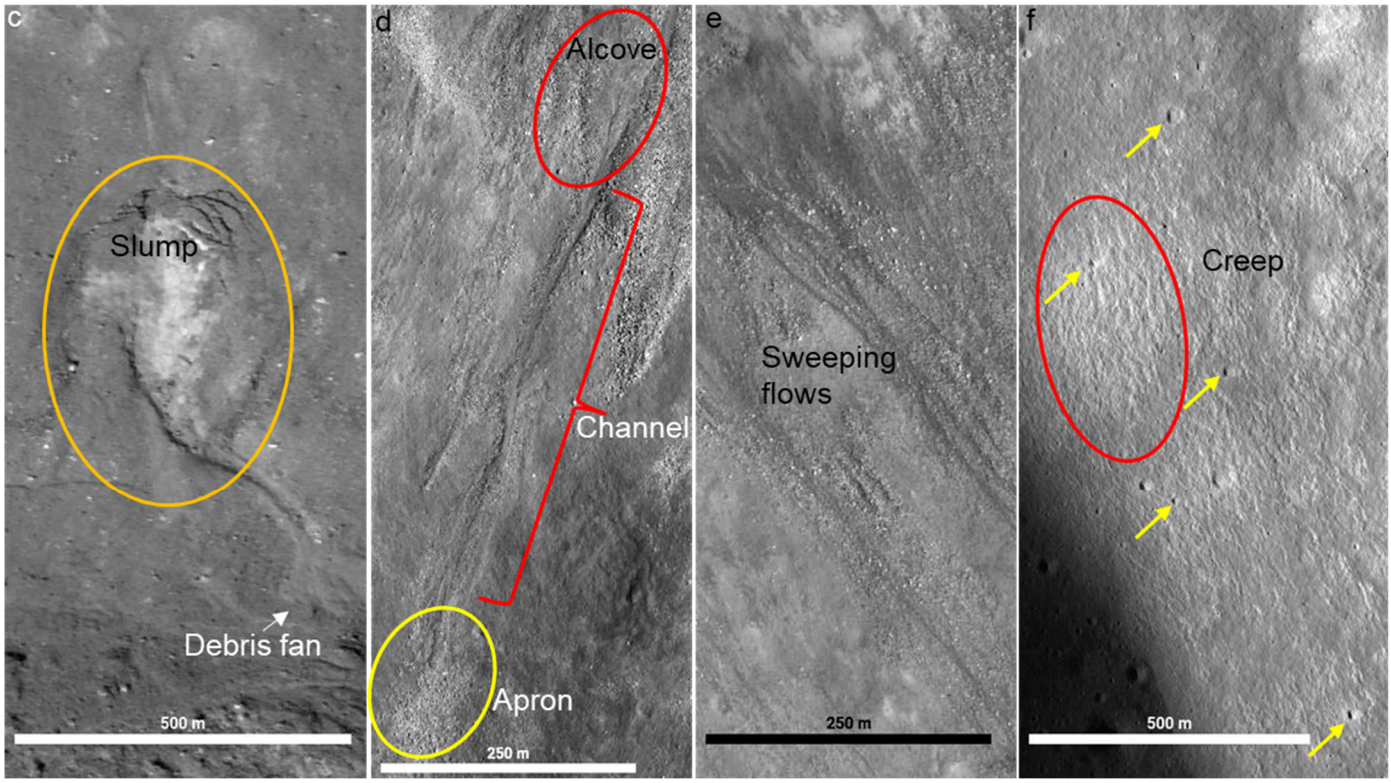

Figure 3. Examples of mass wasting on the Moon (north is up for all the images): (**a**) evidence of rockfalls on the northern wall of the Giordano Bruno Crater (LROC NAC ID: M106209806R, centered at 36° N/103° E). The red rectangle highlights the zoomed-in view of boulder tracks with one lodged boulder; (**b**) rock/debris slides (yellow rectangle) with extensive talus deposits on the western wall of the Aristarchus Crater (LROC NAC ID: M107192593L, centered at 23.7 ° N/312.6° E); (**c**) a well-developed slump (orange ellipse) on the northern wall of the Giordano Bruno Crater (LROC NAC ID: M106209806R, centered at 36° N/103° E); (**d**) an example of channeled flows on the northern wall of the Gambart Crater (LROC NAC ID: M127009259R, centered at 3.4° N/348.21° E). The red ellipse marks the alcove while the yellow ellipse shows the talus apron; (**e**) examples of sweeping flow (dark albedo lineation) on the north-western wall of Dawes Crater (LROC NAC ID: M113785646L, centered at 17.2° N/26.4° E); (**f**) regolith creeping producing rippled topography (red ellipse) on the central peak of Eratosthenes Crater (LROC NAC ID: M117569408R, centered at 14.5° N/348.7° E). The yellow arrows point to several small craters with straightened western walls, deformed as a result of regolith creeping. The maps were generated using the JMARS tool developed by Arizona State University [36].

Mass wasting, being largely a slope phenomenon (~10°–40° slope range for the Moon), causes higher erosion rates leading to larger regolith production on lunar slopes, thus modulating crater densities on slopes and affecting the accuracy of the planetary surface chronology derived through crater counting techniques [2]. Therefore, understanding lunar mass wasting processes is vital for planetary dating, giving us another reason to investigate them further. A spatially more focused study by Kokelaar et al. [14] used LROC-NAC images to interpret scars and deposits formed by mass wasting within seven craters in equatorial (non-polar) latitudes. Kokelaar et al. [14] observed and inferred previously undocumented mass wasting phenomena such as remobilization of stable coarse talus by inundation with fine-grained debris, accumulation of veils of this fine-grained debris around the coarse-grained flow deposits, and the occurrence of long-runout erosion-deposition waves. These findings further highlight the scope of research on lunar mass wasting processes. Identifying other phenomena and subtypes of lunar mass wasting

processes through global-scale inventories can significantly enhance our understanding of planetary landscape evolution under reduced gravity and a scant atmosphere.

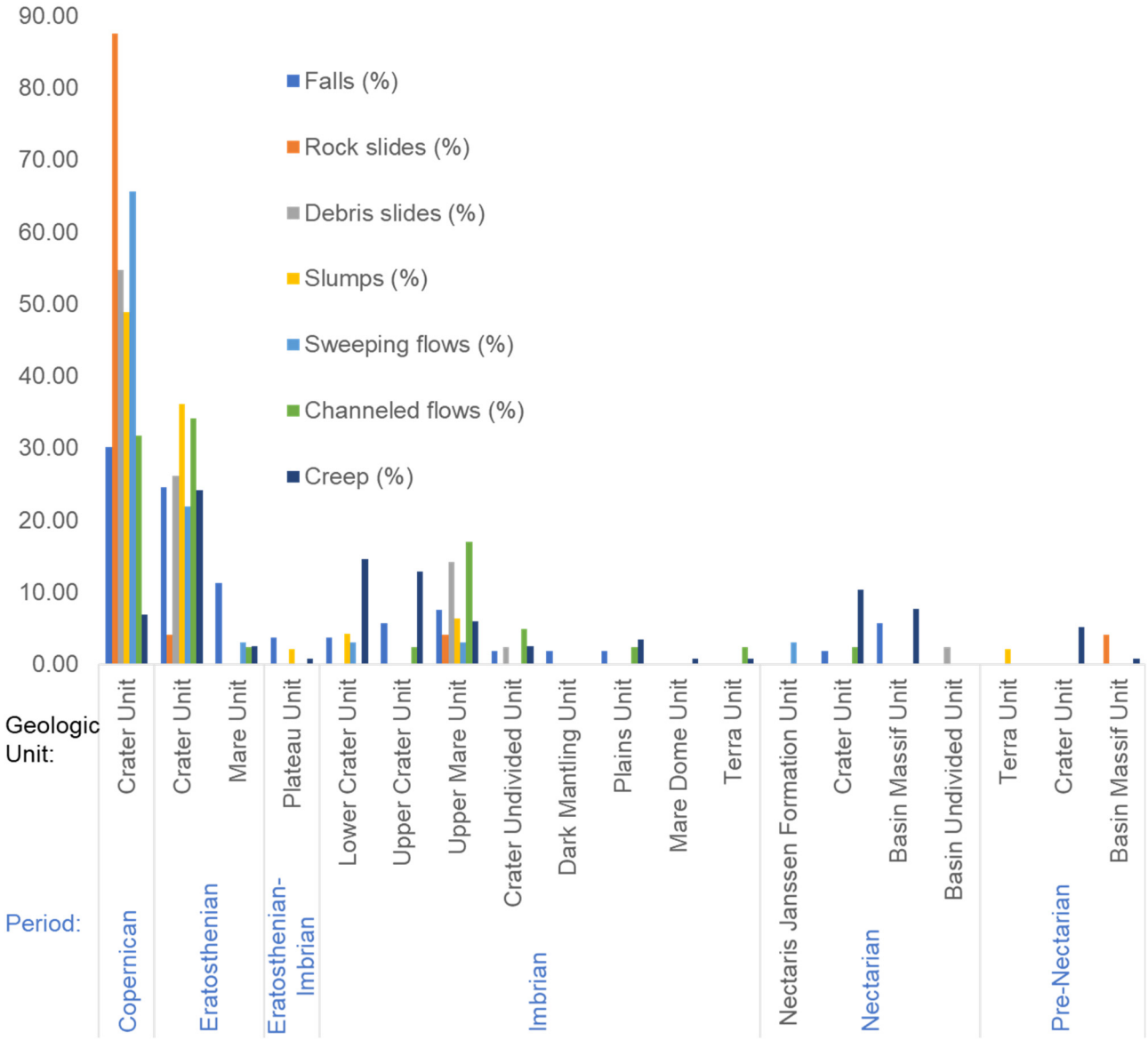

Figure 4. Stratigraphic ages of geologic units hosting lunar mass wasting features, derived using mass wasting data from the Supplementary Material of Xiao et al. [2] and the latest data of lunar geology from the United States Geological Survey [30]. The description of the geologic units can be downloaded from the USGS [41].

2.2. Prospects

In the past couple of years, the focus of various space agencies (e.g., [32,42]) and companies has (re)shifted to lunar research, and the possibility of a permanent lunar base station [43] has further added to the exploratory value of our Moon. The plan seems to be to return to the Moon in 2024, followed by developing a sustained, strategic presence at the lunar South Pole called the Artemis Base Camp. Planned activities at the Artemis Base Camp over the next decade will pave the way to long-term economic and scientific activity at the Moon as well as possible human missions to Mars in subsequent decades. The excess distribution of regolith and boulders on the Moon has largely been defined by mass wasting processes and has long been a concern for engineering [44]. Thus, the motivation to

re-explore the Moon is actually driven not only by the need to improve our understanding of the lunar surface processes through new high-resolution remote sensing datasets, but also by the need to facilitate the exploration of the Solar System beyond the Moon.

As explained above, detailed studies on lunar mass wasting have become possible only in the post-LROC era within the past decade. Thus, there is still a significant amount of research that needs to be carried out to fill the existing gaps in our knowledge of lunar mass wasting processes. Understanding the global distribution of such processes has further geophysical relevance (e.g., [45]). Although numerous mass wasting features have been noticed and reported during the past decade using LROC-NAC images, their morphological and geometrical characteristics, spatial distribution, and age of formation are yet to be systematically studied at the global scale. An important work [27] in this direction was concluded recently where a global inventory of at least one type of lunar mass wasting, i.e., rockfalls, was compiled. The finding of Bickel et al. [27] further confirms that rockfalls are primarily driven by impacts, can also potentially reveal regions of recent seismic activity, and are still present in the oldest, pre-Nectarian topography. These finding signify the relevance of global-scale research as the limited sampling by Xiao et al. [2] had previously revealed the absence of rockfall features in pre-Nectarian terrain. However, there are still other types of reported lunar mass movements, such as debris flows, slides, slumps, and creep, whose global distribution analysis and population-scale characterization are yet to be performed. In other words, there is a degree of incompleteness in the compiled data on the global characterization of all the other lunar mass movement processes. It is worth guessing how much more useful information regarding the lunar surface/subsurface we could derive with the global characterization of all these mass wasting processes. Although mass wasting has affected the surface erosion rate on the Moon and has changed local topography, the relative importance of mass wasting compared with other surface processes, or more importantly their combined effect, on the topography evolution of the Moon is not fully understood at the global scale [2]. Having global datasets for all the mass wasting features could further improve our understanding of shallow moonquakes (e.g., [46]) and the bearing capacity of regolith in both polar (e.g., [47]) and non-polar (e.g., [48]) regions with implications for trafficability and in situ resource utilization (ISRU). Experimental results (e.g., [49]) have shown that regolith might be looser in the polar latitudes of the moon compared with previous lunar landing sites (Figure 1) and the study of mass wasting processes in these polar regions could reveal the trafficability of terrain for future polar missions.

Three recent and extremely important findings regarding the reported [50,51] and modeled [52] water on both permanently shadowed [51] and sunlit [50] surfaces of the Moon have made studying lunar mass wasting processes even more relevant. Lunar mass movement processes have always been linked to dry-granular flows (e.g., [2]). However, spectral modeling shows that some ice-bearing pixels may contain as high as ∼30 wt% of water ice that is intimately mixed with dry regolith [51]. Thus, there is a need to reconsider the involved driving factors for lunar mass movements in the regions where water ice has been reported to exist, be mixed with regolith, or be exposed in shadows. Such a characterization and correlation study could provide us with vital clues regarding the physical characteristics of contemporary lunar water and its present and past contribution to lunar landscape evolution.

3. Cerean Periglacial Landforms and Mass Wasting Processes: Status and Prospects

Within the asteroid belt between Mars and Jupiter, the dwarf planet Ceres offered big surprises when, recently, seven very informative research papers from the Science Team of NASA's Dawn spacecraft were published using its end of the mission datasets. More specifically, the findings implied impact-driven mobilization of deep crustal brines [53], fresh emplacement of salts from these ascending brines [54], cryo-hydrologic processes [55], hydrothermal brine effusion [56], cryo-volcanism [57], gravity anomalies [58], and volatile redistribution [59]. In brief, a generalized conclusion of these papers is that Ceres either is

geologically active in the present, or at least was in the very recent past, with the presence of ice volcanoes, active briny and cryo-surface processes, and surviving pockets of an ancient ocean, all of which make a compelling case to investigate mass wasting features in the periglacial environment of Ceres.

3.1. Status of Our Understanding

Dawn's data show that Ceres might have several regions where briny liquid is seeping out onto its surface [54]. There are also mounds and hills that supposedly formed when ice melted and refroze after an asteroid impact millions of years ago, and their sightings support the idea of the presence of an asteroid-wide cryo-volcanism [57]. The findings of exposed water ice on the surface of Ceres [60], and the possibilities that water could persist on Ceres with vast reserves of water ice, evidenced by the presence of periglacial landforms and landslides (PLLs) (Figure 5), have generated significant interest among the planetary science community [33] owing to their implications for not only understanding the geologic past of our solar system but also for ISRU during future deep space missions.

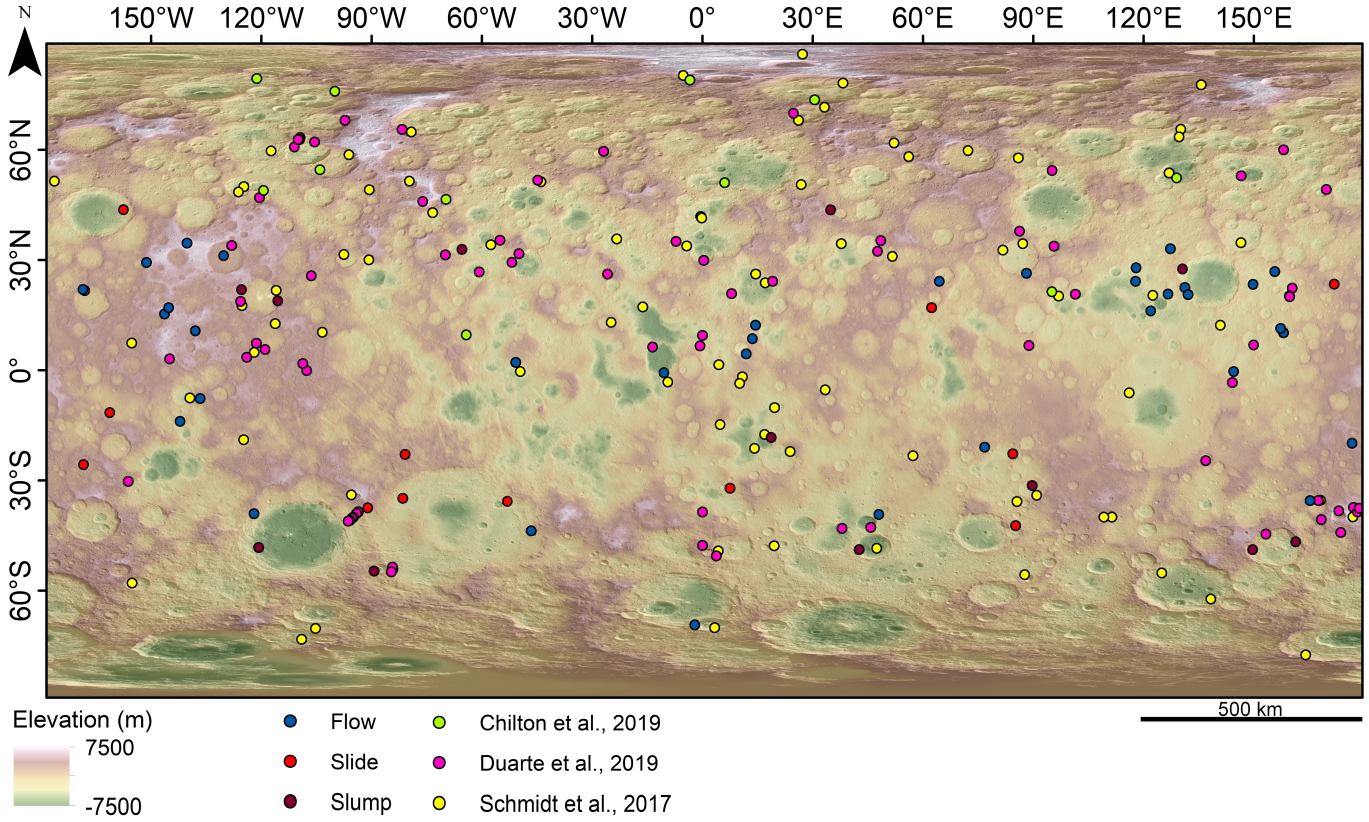

Figure 5. Distribution of identified mass movements on Ceres. The data used to plot this map in GIS were generated by Parkeh et al. [61] and downloaded from Figshare [62]. This map also includes the previously described mass wasting features by Chilton et al. [63], Duarte et al. [64], and Schmidt et al. [65], as compiled by Parekh et al. [61]. The scale is true at the equator.

Periglacial landforms on Ceres have been presented as a subclass of various mass wasting processes observed on the dwarf planet [65]. Furthermore, recent papers (e.g., [63–65]) have investigated the morphological characteristics of Cerean landslides as a sign of the presence, location, and abundance of ground ice. Schmidt et al. [65] provided the first analysis of mass wasting slides on Ceres (Figure 5) and characterized them into three morphological types. Type 1 slides, located at high latitudes on Ceres, display a furrowed topography with a thick lobate terminus [65]. They are the most stagnant type of slide on Ceres [65]. The furrowed and lobate topography gives them an appearance similar to terrestrial rock glaciers and

icy landslides [65]. The most commonly sighted slides on Ceres, i.e., Type 2 slides, have intermediate mobility and are longer than Type 1 slides. Their topography is sheet-like with thin termini [65]. Terrestrial avalanche deposits can be taken as geomorphologic analogues of Type 2 slide deposits on Ceres. Type 3 slides have the highest mobility, and, hence, a long runout and a platy lobate morphology [65]. The high mobility and the formation of Type 3 slides might be attributed to some involvement of transiently melting ice within the regolith, giving them a mudflow-like morphology [65]. The Tsiolkovskiy long-runout landslide on the Moon [66] is an appropriate morphological analogue for Type 3 Cerean slides [65]. These landslides are always associated with large impact craters, and due to their morphological resemblance to ejected material from craters in the icy regions of Mars and on Jupiter's moon Ganymede, they are postulated to have formed when an impact event melted subsurface ice on Ceres. Based on the lack of clear trends between mobility and slide volume, and drawing parallels with the findings of Singer et al. [67], Schmidt et al. [65] argued that ice played an important role in determining the mobility of Cerean slides. Schmidt et al. [65] also acknowledge the presence of more slides, specifically Type 1 slides, at the polar latitudes of Ceres, and such a spatial distribution coupled with the morphological inferences indicate a substantial amount of ice in the shallow subsurface. These conclusions were further investigated and broadly accepted by detailed follow-up analyses by Chilton et al. [63] and Duarte et al. [64].

A recent paper [61] throws more light on mass wasting processes on Ceres. Parekh et al.'s global mass movement classification [61] was more holistic in terms of identifying very diverse mass wasting features (Figure 5) and comparing them with similar features on Vesta with a different dry regolith. Parekh et al. [61] focused on three common morphology types: (1) flow-like movements (Figure 6a,b) as either lobate features or as large and thin sheet-like fans; (2) slides (Figure 6c) showing granular flow behavior; and (3) slumps (Figure 6d) as collapsed unconsolidated material. Based on the availability of digital terrain models (DTMs) of a suitable resolution, Parekh et al. [61] also performed a profile analysis for 34 out of a total of 210 identified mass wasting features on Ceres, and did not observe a correlation between crater size and abundance of mass wasting features.

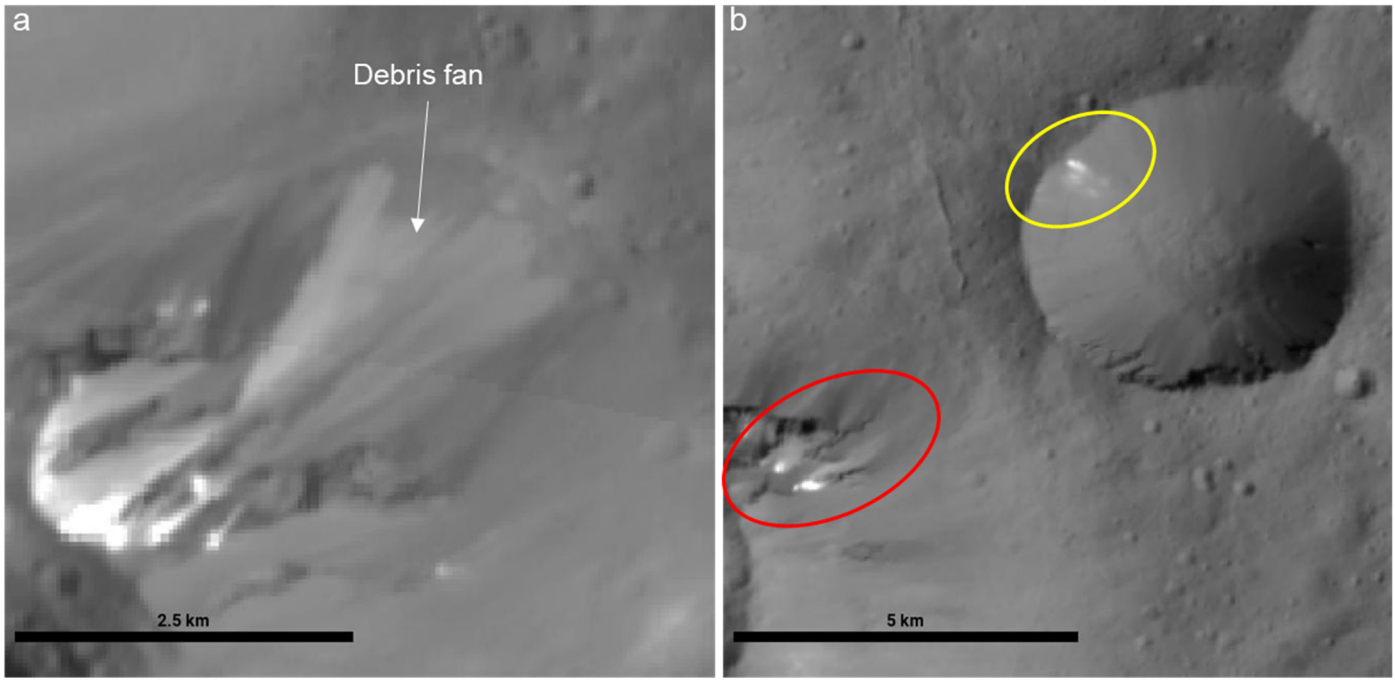

Figure 6. *Cont.*

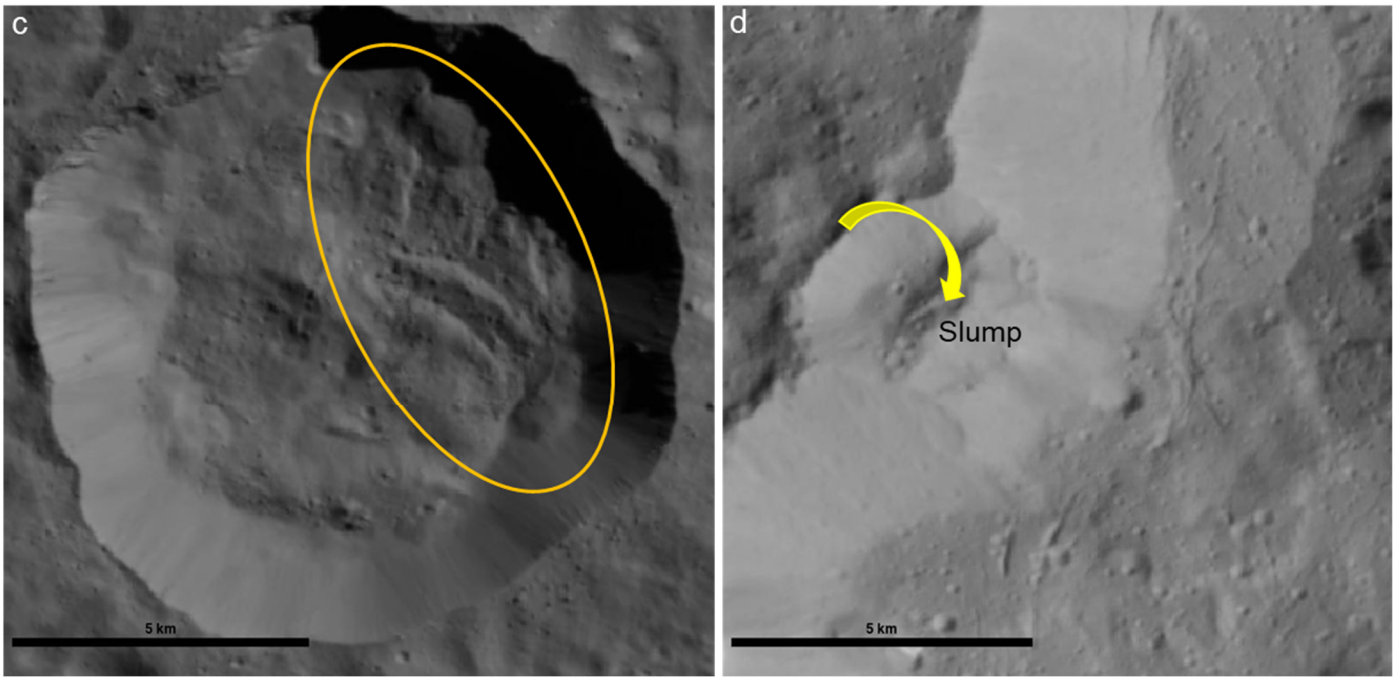

Figure 6. Examples of mass wasting features of Ceres (north is up for all the images): (**a**) a flow feature with a well-developed debris fan on the western wall of Dantu Crater (26.375° N, 137.281° E); (**b**) a flow feature (red ellipse) on the western wall of Dantu Crater and an undocumented possible flow candidate (yellow ellipse) on the north-western wall of Axomama Crater; (**c**) slide deposits on the floor of an unnamed crater (−25.828° N, 191.58° E); (**d**) a slump feature on the western wall of Dantu Crater. The yellow curved arrow shows the topographic displacement downwards. The maps were generated using the JMARS tool developed by Arizona State University [36].

3.2. Prospects

The new observations of hydrological, periglacial, and mass wasting processes on Ceres that resemble those on Earth, Mars, and the Moon have been influenced by the crustal composition of Ceres [59]. These processes are also expected to act on icy satellites [59]. Hence, these Dawn observations of Cerean PLLs warrant detailed exploration in order to establish Ceres as a "cryo-analogue" for icy moons and asteroids. This could also help prepare for the interpretation of future observations of icy moons from the missions planned for the coming decade [33], in particular for Europa (the Europa Clipper mission) and Ganymede (the Jupiter Icy moons explorer (JUICE)). Recently, a 130-km-long lobate feature on the Uranian satellite Ariel was extensively explored using Voyager 2's Imaging Science System (ISS) images and DTM, and a cryo-volcanic origin was suggested [68]. More importantly, this result suggests the possibility that Ariel is, or was, also an ocean world [68]. In the planet-wide icy environment of Pluto, sublimation has been suggested to be a landform-shaping process driving various types of mass wasting [69]. Understanding heat and material transfer in a brine–rock mixture and in a fractured crust under reduced gravity conditions is crucial to exploring the geomorphology and habitability of mid-sized ocean worlds and the PLL features on Ceres may act as viable analogues to develop needed theoretical frameworks [33]. Drawing inferences from detailed global-scale geomorphometry of mass wasting features on Ceres could be useful in understanding the dynamics of ice–debris complexes on such icy dwarf planets, asteroids, and moons.

Thanks to all these excellent results published in recent years using Dawn data, our understanding of the surface–subsurface processes on Ceres has considerably improved. However, in terms of studying mass wasting on Ceres, there remain ample opportunities.

First, Parekh et al.'s results [61] highlight that with dedicated geomorphology observations, there is a possibility to identify and add more mass wasting features to the existing inventories (e.g., [61,63–65]). Parekh et al. [61] do not claim that their inventory of Cerean

mass wasting features is globally complete as they were more inclined to identify broad mass wasting categories that were comparable between Ceres and Vesta. Indeed, the yellow ellipse in Figure 6b shows a yet-to-be-documented potential flow feature in the 5-km-wide Axomama Crater. Therefore, identifying more distinct subclasses of characterized mass wasting features on Ceres is still possible and could reveal further details on mass wasting processes under reduced gravity conditions and in periglacial environments.

Second, all the available mass wasting inventories for Ceres compile drop height and runout length as the primary terrain parameters. On the other hand, in terrestrial contexts, outlines, cross-sectional widths, and estimated areas of these features are considered to be equally important parameters to take into account while studying their formation and rheology [70]. Further efforts in incorporating these additional parameters into existing inventories could help build a holistic database for the community.

Third, a recent study [71] has argued that landslide morphology cannot be used to draw conclusions about local ice content and composition, and terrain and topography play a bigger role in defining the characteristics of periglacial features and landslides on Ceres. A similar conclusion was recently published [72] for Martian landslides with a focus on studying and understanding the local topography. Another recent study [73] in a terrestrial context has also highlighted the importance of geomorphometric analyses for mass wasting features in understanding their genesis. Such morphometric analyses for Cerean landslides, including estimation of parameters such as slope, aspect, curvature, and roughness, should also be performed and included in the global inventory.

Fourth, another recent study [74] very interestingly provided evidence of variations in the amount of water ice on Ceres' surface, suggesting a seasonal water cycle. This seasonal increase in water ice covers up to ~2 km^2 more of the area in a mid-latitude crater. The observed increase, coupled with Ceres' orbital parameters, points to an ongoing process that seems to be correlated with solar flux [74]. We believe that such a seasonal enrichment of regolith with water ice is equivalent to the seasonal water enrichment within terrestrial rock glaciers [75], which eventually controls their flow/dynamics. Therefore, feature tracking analysis (e.g., [76,77]) using the available repeat images for larger mass wasting features, particularly slides, could tell us about any contemporary seasonal dynamics in them.

4. Conclusions

In this concept article, we have briefly reviewed the status of mass wasting research on the Moon and Ceres. We have identified key advances made in this direction. We have further highlighted some areas of prospective research that could further enhance our understanding of mass wasting processes under reduced gravity and a scant atmosphere. The next couple of decades are bound to witness unforeseen advances in the exploration of our Solar System, and both the Moon and Ceres hold unique significance in facilitating that exploration. While the Moon can offer ISRU opportunities for exploring inner Solar System bodies, Ceres, as the main base and transit hub for asteroid mining, can serve a similar purpose for future deep space exploration. As explained in this article, a better understanding of mass wasting features and related geomorphologies could help us assess rover trafficability and the bearing capacity of regolith, understand physical characteristics of contemporary lunar water and ice content in Cerean regolith, and assess seasonal dynamics in Cerean PLLs. The available remote sensing data for the Moon and Ceres should be sufficient to explore all the prospective themes within this article, and the results should be able to better inform the space agencies on needed future remote sensing missions.

Author Contributions: Conceptualization, L.S. and A.B.; methodology, L.S. and A.B.; software, L.S. and A.B.; validation, L.S. and A.B.; formal analysis, L.S. and A.B.; investigation, L.S. and A.B.; resources, L.S. and A.B.; writing—original draft preparation, L.S.; writing—review and editing, A.B.; visualization, A.B. and L.S. All authors have read and agreed to the published version of the manuscript.

Funding: This research received no external funding.

Institutional Review Board Statement: Not applicable.

Informed Consent Statement: Not applicable.

Data Availability Statement: Not applicable.

Acknowledgments: All the data sources have been credited in the respective figure captions. However, we thank ETH Zurich's Research Collection, the United States Geological Survey, previous studies [2,27,30,61,62], and Arizona State University for providing the necessary datasets and tools, which we have used to generate various figures and maps in this study.

Conflicts of Interest: The authors declare no conflict of interest.

References

1. Varnes, D.J. *Landslide Hazard Zonation: A Review of Principles and Practice*; UNESCO Press: Paris, France, 1984; ISBN 978-92-3-101895-4.
2. Xiao, Z.; Zeng, Z.; Ding, N.; Molaro, J. Mass wasting features on the moon—How active is the lunar surface? *Earth Planet. Sci. Lett.* **2013**, *376*, 1–11. [CrossRef]
3. Chen, Q.; Zhang, S.; Chang, S.; Liu, B.; Liu, J.; Long, J. Geophysical interpretation of a subsurface landslide in the Southern Qinshui basin. *J. Environ. Eng. Geophys.* **2019**, *24*, 433–449. [CrossRef]
4. Corsini, A.; Borgatti, L.; Cervi, F.; Dahne, A.; Ronchetti, F.; Sterzai, P. Estimating mass-wasting processes in active earth slides—Earth flows with time-series of high-resolution DEMs from photogrammetry and airborne LiDAR. *Nat. Hazards Earth Syst. Sci.* **2009**, *9*, 433–439. [CrossRef]
5. Deplus, C.; Le Friant, A.; Boudon, G.; Komorowski, J.-C.; Villemant, B.; Harford, C.; Ségoufin, J.; Cheminée, J.-L. Submarine evidence for large-scale debris avalanches in the lesser Antilles arc. *Earth Planet Sci. Lett.* **2001**, *192*, 145–157. [CrossRef]
6. Moore, J.G.; Normark, W.R.; Holcomb, R.T. Giant Hawaiian landslides. *Annu. Rev. Earth Planet Sci.* **1994**, *22*, 119–144. [CrossRef]
7. Parker, R.N.; Densmore, A.L.; Rosser, N.J.; de Michele, M.; Li, Y.; Huang, R.; Whadcoat, S.; Petley, D.N. Mass wasting triggered by the 2008 wenchuan earthquake is greater than orogenic growth. *Nat. Geosci.* **2011**, *4*, 449–452. [CrossRef]
8. Bhardwaj, S.A.; Pandit, A.; Ganju, A. Demarcation of potential avalanche sites using remote sensing and ground observations: A case study of Gangotri Glacier. *Geocarto Int.* **2014**, *29*, 520–535. [CrossRef]
9. Wolman, M.G.; Gerson, R. Relative scales of time and effectiveness of climate in watershed geomorphology. *Earth Surf. Process.* **1978**, *3*, 189–208. [CrossRef]
10. Casagli, N.; Frodella, W.; Morelli, S.; Tofani, V.; Ciampalini, A.; Intrieri, E.; Raspini, F.; Rossi, G.; Tanteri, L.; Lu, P. Spaceborne, UAV and ground-based remote sensing techniques for landslide mapping, monitoring and early warning. *Geoenviron. Disasters* **2017**, *4*, 9. [CrossRef]
11. Kyriou, A.; Nikolakopoulos, K.; Koukouvelas, I. How image acquisition geometry of UAV campaigns affects the derived products and their accuracy in areas with complex geomorphology. *ISPRS Int. J. Geoinf.* **2021**, *10*, 408. [CrossRef]
12. Ritter, D.F.; Kochel, R.C.; Miller, J.R. *Process Geomorphology*; Waveland Press: Long Grove, IL, USA, 2006.
13. Solari, L.; Del Soldato, M.; Raspini, F.; Barra, A.; Bianchini, S.; Confuorto, P.; Casagli, N.; Crosetto, M. Review of satellite interferometry for landslide detection in Italy. *Remote Sens.* **2020**, *12*, 1351. [CrossRef]
14. Kokelaar, B.P.; Bahia, R.S.; Joy, K.H.; Viroulet, S.; Gray, J.M.N.T. Granular avalanches on the moon: Mass-wasting conditions, processes, and features. *J. Geophys. Res. Planets* **2017**, *122*, 1893–1925. [CrossRef]
15. Brunetti, M.T.; Xiao, Z.; Komatsu, G.; Peruccacci, S.; Guzzetti, F. Large rock slides in impact craters on the moon and mercury. *Icarus* **2015**, *260*, 289–300. [CrossRef]
16. Waltham, D.; Pickering, K.T.; Bray, V.J. Particulate gravity currents on Venus. *J. Geophys. Res. Planets* **2008**, *113*, E02012. [CrossRef]
17. Bhardwaj, A.; Sam, L.; Martín-Torres, F.J.; Zorzano, M.-P.; Fonseca, R.M. Martian slope streaks as plausible indicators of transient water activity. *Sci. Rep.* **2017**, *7*, 7074. [CrossRef] [PubMed]
18. Bhardwaj, A.; Sam, L.; Martín-Torres, F.J.; Zorzano, M.-P. Are slope streaks indicative of global-scale aqueous processes on contemporary mars? *Rev. Geophys.* **2019**, *57*, 48–77. [CrossRef]
19. Bhardwaj, A.; Sam, L.; Martín-Torres, F.J.; Zorzano, M.-P. Discovery of recurring slope lineae candidates in Mawrth Vallis, Mars. *Sci. Rep.* **2019**, *9*, 2040. [CrossRef] [PubMed]
20. Bhardwaj, A.; Sam, L.; Gharehchahi, S. Four decades of understanding martian geomorphology: Revisiting Baker's 'The Geomorphology of Mars'. *Prog. Phys. Geogr. Earth Environ.* **2021**, *45*, 979–989. [CrossRef]
21. McEwen, A.S. Mobility of large rock avalanches: Evidence from Valles Marineris, Mars. *Geology* **1989**, *17*, 1111–1114. [CrossRef]
22. Schenk, P.M.; Bulmer, M.H. Origin of mountains on io by thrust faulting and large-scale mass movements. *Science* **1998**, *279*, 1514–1517. [CrossRef]
23. Hall, S. The race to Venus. *Nature* **2019**, *570*, 20–25. [CrossRef] [PubMed]
24. Pradhan, S.P.; Siddique, T. Mass wasting: An overview. In *Landslides: Theory, Practice and Modelling*; Pradhan, S.P., Vishal, V., Singh, T.N., Eds.; Springer International Publishing: Berlin/Heidelberg, Germany, 2019; pp. 3–20, ISBN 978-3-319-77377-3.
25. Bhardwaj, A.; Sam, L. Reconstruction and characterisation of past and the most recent slope failure events at the 2021 rock-ice avalanche site in Chamoli, Indian Himalaya. *Remote Sens.* **2022**, *14*, 949. [CrossRef]

26. Corominas, J.; van Westen, C.; Frattini, P.; Cascini, L.; Malet, J.-P.; Fotopoulou, S.; Catani, F.; Van Den Eeckhaut, M.; Mavrouli, O.; Agliardi, F.; et al. Recommendations for the quantitative analysis of landslide risk. *Bull. Eng. Geol. Environ.* **2014**, *73*, 209–263. [CrossRef]
27. Bickel, V.T.; Aaron, J.; Manconi, A.; Loew, S.; Mall, U. Impacts drive lunar rockfalls over billions of years. *Nat. Commun.* **2020**, *11*, 2862. [CrossRef]
28. Characterised Lunar Rockfalls. ETH Zurich Research Collection. Available online: https://www.research-collection.ethz.ch/; (accessed on 1 January 2022).
29. Unified Geologic Map of the Moon. United States Geological Survey. Available online: https://astrogeology.usgs.gov/search/map/Moon/Geology/Unified_Geologic_Map_of_the_Moon_GIS_v2 (accessed on 1 January 2022).
30. Fortezzo, C.M.; Spudis, P.D.; Harrel, S.L. *Release of the Digital Unified Global Geologic Map of the Moon at 1:5,000,000-Scale*; Lunar and Planetary Institute: Houston, TX, USA, 2020; p. 2760.
31. Estes, N.M.; Robinson, M.S. LROC: Ten Years Exploring the Moon. In Proceedings of the 4th Planetary Data Workshop, Flagstaff, AZ, USA, 18–20 June 2019; Volume 2151, p. 7082.
32. Li, C.; Wang, C.; Wei, Y.; Lin, Y. China's present and future lunar exploration program. *Science* **2019**, *365*, 238–239. [CrossRef]
33. Castillo-Rogez, J. Future exploration of ceres as an ocean world. *Nat. Astron.* **2020**, *4*, 732–734. [CrossRef]
34. Lindsay, J.F. Energy at the lunar surfaces. In *Lunar Stratigraphy and Sedimentology*; Kopal, Z., Cameron, A.G.W., Eds.; Elsevier: Amsterdam, The Netherlands, 1976; Volume 3, pp. 45–55, ISBN 978-0-444-41443-4.
35. Pike, R.J. Some preliminary interpretations of lunar mass-wasting processes from Apollo 10 photography. In *Analysis of Apollo 10 Photography and Visual Observations, NASA Special Publication, NASA-SP-232*; NASA: Washington, DC, USA, 1971; Volume 232, pp. 14–20.
36. JMARS Tool Developed by Arizona State University. Available online: http://jmars.asu.edu/ (accessed on 27 December 2021).
37. Melosh, H.J. The mechanics of large rock avalanches. In *Debris Flows/Avalanches: Process, Recognition, and Mitigation*; Costa, E.J., Wieczorek, G.F., Eds.; Geological Society of America: Boulder, CO, USA, 1987; Volume 7, pp. 41–50.
38. Kleinhans, M.G.; Markies, H.; de Vet, S.J.; in't Veld, A.C.; Postema, F.N. Static and dynamic angles of repose in loose granular materials under reduced gravity. *J. Geophys. Res. Planets* **2011**, *116*, E11. [CrossRef]
39. Losiak, A.; Wilhelms, D.E.; Byrne, C.J.; Thaisen, K.G.; Weider, S.Z.; Kohout, T.; O'Sullivan, K.; Kring, D.A. A new lunar impact crater database. In Proceedings of the 40th Lunar and Planetary Science Conference, (Lunar and Planetary Science XL), The Woodlands, TX, USA, 23–27 March 2009; p. 1532.
40. Wilhelms, D.E.; McCauley, J.F.; Trask, N.J. *The Geologic History of the Moon*; Professional Paper 1348; United States Government Printing Office: Washington, DC, USA, 1987.
41. Geological Units Description. Available online: https://astropedia.astrogeology.usgs.gov/download/Moon/Geology/thumbs/UnifiedGeologicMapofTheMoon200dpi.jpg (accessed on 1 January 2022).
42. Chavers, G.; Watson-Morgan, L.; Smith, M.; Suzuki, N.; Polsgrove, T. NASA's human landing system: The strategy for the 2024 mission and future sustainability. In Proceedings of the 2020 IEEE Aerospace Conference, Big Sky, MT, USA, 7–14 March 2020; pp. 1–9.
43. NASA's Plan for Sustained Lunar Exploration and Development. Available online: https://www.nasa.gov/sites/default/files/atoms/files/a_sustained_lunar_presence_nspc_report4220final.pdf (accessed on 27 December 2021).
44. Berger, K.J.; Anand, A.; Metzger, P.T.; Hrenya, C.M. Role of collisions in erosion of regolith during a lunar landing. *Phys. Rev. E* **2013**, *87*, 22205. [CrossRef]
45. Bandfield, J.L.; Ghent, R.R.; Vasavada, A.R.; Paige, D.A.; Lawrence, S.J.; Robinson, M.S. Lunar surface rock abundance and regolith fines temperatures derived from LRO diviner radiometer data. *J. Geophys. Res. Planets* **2011**, *116*, E00H02. [CrossRef]
46. 46. Senthil Kumar, P.; Sruthi, U.; Krishna, N.; Lakshmi, K.J.P.; Menon, R.; Amitabh, B.; Gopala Krishna, B.; Kring, D.A.; Head, J.W.; Goswami, J.N.; et al. Recent shallow moonquake and impact-triggered boulder falls on the moon: New insights from the Schrödinger basin. *J. Geophys. Res. Planets* **2016**, *121*, 147–179. [CrossRef]
47. Sargeant, H.M.; Bickel, V.T.; Honniball, C.I.; Martinez, S.N.; Rogaski, A.; Bell, S.K.; Czaplinski, E.C.; Farrant, B.E.; Harrington, E.M.; Tolometti, G.D.; et al. Using boulder tracks as a tool to understand the bearing capacity of permanently shadowed regions of the moon. *J. Geophys. Res. Planets* **2020**, *125*, e2019JE006157. [CrossRef]
48. Bickel, V.T.; Honniball, C.I.; Martinez, S.N.; Rogaski, A.; Sargeant, H.M.; Bell, S.K.; Czaplinski, E.C.; Farrant, B.E.; Harrington, E.M.; Tolometti, G.D.; et al. Analysis of lunar boulder tracks: Implications for trafficability of pyroclastic deposits. *J. Geophys. Res. Planets* **2019**, *124*, 1296–1314. [CrossRef]
49. Metzger, P.T.; Anderson, S.; Colaprete, A. *Experiments Indicate Regolith is Looser in the Lunar Polar Regions Than at the Lunar Landing Sites*; American Society of Civil Engineers: Reston, VA, USA, 2018; pp. 79–85.
50. Honniball, C.I.; Lucey, P.G.; Li, S.; Shenoy, S.; Orlando, T.M.; Hibbitts, C.A.; Hurley, D.M.; Farrell, W.M. Molecular water detected on the sunlit moon by SOFIA. *Nat. Astron.* **2021**, *5*, 121–127. [CrossRef]
51. Li, S.; Lucey, P.G.; Milliken, R.E.; Hayne, P.O.; Fisher, E.; Williams, J.-P.; Hurley, D.M.; Elphic, R.C. Direct evidence of surface exposed water ice in the lunar polar regions. *Proc. Natl. Acad. Sci. USA* **2018**, *115*, 8907–8912. [CrossRef]
52. Schorghofer, N.; Williams, J.-P. Mapping of ice storage processes on the moon with time-dependent temperatures. *Planet Sci. J.* **2020**, *1*, 54. [CrossRef]

53. Raymond, C.A.; Ermakov, A.I.; Castillo-Rogez, J.C.; Marchi, S.; Johnson, B.C.; Hesse, M.A.; Scully, J.E.C.; Buczkowski, D.L.; Sizemore, H.G.; Schenk, P.M.; et al. Impact-driven mobilization of deep crustal brines on dwarf planet ceres. *Nat. Astron.* **2020**, *4*, 741–747. [CrossRef]
54. De Sanctis, M.C.; Ammannito, E.; Raponi, A.; Frigeri, A.; Ferrari, M.; Carrozzo, F.G.; Ciarniello, M.; Formisano, M.; Rousseau, B.; Tosi, F.; et al. Fresh emplacement of hydrated sodium chloride on ceres from ascending salty fluids. *Nat. Astron.* **2020**, *4*, 786–793. [CrossRef]
55. Schmidt, B.E.; Sizemore, H.G.; Hughson, K.H.G.; Duarte, K.D.; Romero, V.N.; Scully, J.E.C.; Schenk, P.M.; Buczkowski, D.L.; Williams, D.A.; Nathues, A.; et al. Post-impact cryo-hydrologic formation of small mounds and hills in ceres's occator crater. *Nat. Geosci.* **2020**, *13*, 605–610. [CrossRef]
56. Scully, J.E.C.; Schenk, P.M.; Castillo-Rogez, J.C.; Buczkowski, D.L.; Williams, D.A.; Pasckert, J.H.; Duarte, K.D.; Romero, V.N.; Quick, L.C.; Sori, M.M.; et al. The varied sources of faculae-forming brines in ceres' occator crater emplaced via hydrothermal brine effusion. *Nat. Commun.* **2020**, *11*, 3680. [CrossRef]
57. Nathues, A.; Schmedemann, N.; Thangjam, G.; Pasckert, J.H.; Mengel, K.; Castillo-Rogez, J.; Cloutis, E.A.; Hiesinger, H.; Hoffmann, M.; Le Corre, L.; et al. Recent cryovolcanic activity at occator crater on ceres. *Nat. Astron.* **2020**, *4*, 794–801. [CrossRef]
58. Park, R.S.; Konopliv, A.S.; Ermakov, A.I.; Castillo-Rogez, J.C.; Fu, R.R.; Hughson, K.H.G.; Prettyman, T.H.; Raymond, C.A.; Scully, J.E.C.; Sizemore, H.G.; et al. Evidence of non-uniform crust of ceres from dawn's high-resolution gravity data. *Nat. Astron.* **2020**, *4*, 748–755. [CrossRef]
59. Schenk, P.; Scully, J.; Buczkowski, D.; Sizemore, H.; Schmidt, B.; Pieters, C.; Neesemann, A.; O'Brien, D.; Marchi, S.; Williams, D.; et al. Impact heat driven volatile redistribution at occator crater on ceres as a comparative planetary process. *Nat. Commun.* **2020**, *11*, 3679. [CrossRef] [PubMed]
60. Combe, J.-P.; McCord, T.B.; Tosi, F.; Ammannito, E.; Carrozzo, F.G.; De Sanctis, M.C.; Raponi, A.; Byrne, S.; Landis, M.E.; Hughson, K.H.G.; et al. Detection of local H2O exposed at the surface of ceres. *Science* **2016**, *353*, aaf3010. [CrossRef] [PubMed]
61. Parekh, R.; Otto, K.A.; Jaumann, R.; Matz, K.D.; Roatsch, T.; Kersten, E.; Elgner, S.; Raymond, C. Influence of volatiles on mass wasting processes on vesta and ceres. *JGR Planets* **2021**, *126*, e2020JE006573. [CrossRef]
62. Parekh, R. Data for "Influence of Volatiles on Mass Wasting Processes on Vesta and Ceres".7z. *J. Contrib.* **2020**. [CrossRef]
63. Chilton, H.T.; Schmidt, B.E.; Duarte, K.; Ferrier, K.L.; Hughson, K.H.G.; Scully, J.E.C.; Wray, J.J.; Sizemore, H.G.; Nathues, A.; Platz, T.; et al. Landslides on ceres: Inferences into ice content and layering in the upper crust. *J. Geophys. Res. Planets* **2019**, *124*, 1512–1524. [CrossRef]
64. Duarte, K.D.; Schmidt, B.E.; Chilton, H.T.; Hughson, K.H.G.; Sizemore, H.G.; Ferrier, K.L.; Buffo, J.J.; Scully, J.E.C.; Nathues, A.; Platz, T.; et al. Landslides on ceres: Diversity and geologic context. *J. Geophys. Res. Planets* **2019**, *124*, 3329–3343. [CrossRef]
65. Schmidt, B.E.; Hughson, K.H.G.; Chilton, H.T.; Scully, J.E.C.; Platz, T.; Nathues, A.; Sizemore, H.; Bland, M.T.; Byrne, S.; Marchi, S.; et al. Geomorphological evidence for ground ice on dwarf planet ceres. *Nat. Geosci.* **2017**, *10*, 338–343. [CrossRef]
66. Boyce, J.M.; Mouginis-Mark, P.; Robinson, M. The Tsiolkovsky crater landslide, the moon: An LROC view. *Icarus* **2020**, *337*, 113464. [CrossRef]
67. Singer, K.N.; McKinnon, W.B.; Schenk, P.M.; Moore, J.M. Massive ice avalanches on iapetus mobilized by friction reduction during flash heating. *Nat. Geosci.* **2012**, *5*, 574–578. [CrossRef]
68. Beddingfield, C.B.; Cartwright, R.J. A lobate feature adjacent to a double ridge on ariel: Formed by cryovolcanism or mass wasting? *Icarus* **2021**, *367*, 114583. [CrossRef]
69. Moore, J.M.; Howard, A.D.; Umurhan, O.M.; White, O.L.; Schenk, P.M.; Beyer, R.A.; McKinnon, W.B.; Spencer, J.R.; Grundy, W.M.; Lauer, T.R.; et al. Sublimation as a landform-shaping process on Pluto. *Icarus* **2017**, *287*, 320–333. [CrossRef]
70. Kofler, C.; Steger, S.; Mair, V.; Zebisch, M.; Comiti, F.; Schneiderbauer, S. An inventory-driven rock glacier status model (intact vs. relict) for South Tyrol, Eastern Italian Alps. *Geomorphology* **2020**, *350*, 106887. [CrossRef]
71. Johnson, B.C.; Sori, M.M. Landslide morphology and mobility on ceres controlled by topography. *J. Geophys. Res. Planets* **2020**, *125*, e2020JE006640. [CrossRef]
72. Magnarini, G.; Mitchell, T.M.; Grindrod, P.M.; Goren, L.; Schmitt, H.H. Longitudinal ridges imparted by high-speed granular flow mechanisms in martian landslides. *Nat. Commun.* **2019**, *10*, 4711. [CrossRef] [PubMed]
73. Chang, K.-T.; Merghadi, A.; Yunus, A.P.; Pham, B.T.; Dou, J. Evaluating scale effects of topographic variables in landslide susceptibility models using GIS-based machine learning techniques. *Sci Rep.* **2019**, *9*, 12296. [CrossRef]
74. Raponi, A.; De Sanctis, M.C.; Frigeri, A.; Ammannito, E.; Ciarniello, M.; Formisano, M.; Combe, J.-P.; Magni, G.; Tosi, F.; Carrozzo, F.G.; et al. Variations in the amount of water ice on ceres' surface suggest a seasonal water cycle. *Sci. Adv.* **2018**, *4*, eaao3757. [CrossRef]
75. Jones, D.B.; Harrison, S.; Anderson, K.; Whalley, W.B. Rock glaciers and mountain hydrology: A review. *Earth Sci. Rev.* **2019**, *193*, 66–90. [CrossRef]
76. Sam, L.; Gahlot, N.; Prusty, B.G. Estimation of dune celerity and sand flux in part of west Rajasthan, Gadra area of the Thar desert using temporal remote sensing data. *Arab. J. Geosci.* **2015**, *8*, 295–306. [CrossRef]
77. Sam, L.; Bhardwaj, A.; Singh, S.; Kumar, R. Remote sensing flow velocity of debris-covered glaciers using Landsat 8 data. *Prog. Phys. Geogr. Earth Environ.* **2016**, *40*, 305–321. [CrossRef]